

## **Supplementary figure legend**

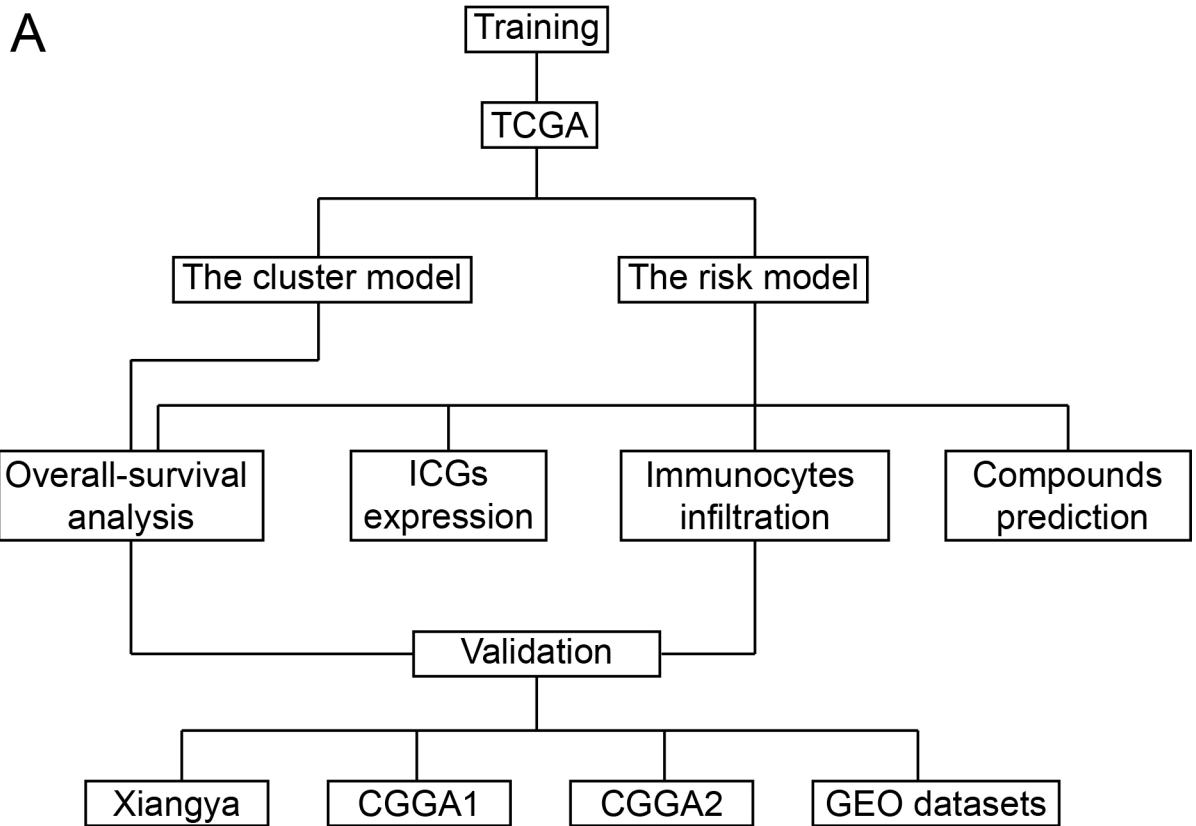
**Supplementary figure 1.** The flow chart and the construction of the cluster model. (A) The flow chart of this study. (B-D) The construction of the cluster model. (E) The PCA diagram of the cluster model. (F) Characteristic of the cluster model learning by employing support vector machine algorithm.

**Supplementary figure 2.** The distribution of the risk model. The distribution of the risk model in gliomas pathological grade (A-B), cancer type (C-D), IDH status (E-F), 1p19q status (G-H), MGMT status (I-J) in the CGGA1 and CGGA2 cohort. NS, not significant, \*\* $p < 0.01$ , \*\*\* $p < 0.001$ .

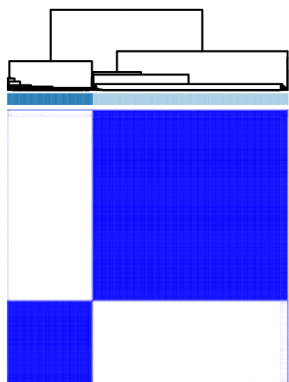
**Supplementary figure 3.** The OS analysis in LGG and GBM. The survival outcome difference between high and low risk group from the LGG and GBM group in the TCGA (A-B), CGGA1 (C-D) and CGGA2 datasets (E-F).

**Supplementary figure 4.** Results from ESTIMATE algorithm and immunocytes infiltration ratio in validation cohort. The distribution of IMMUNEScore, STROMALscore, ESTIMATEScore and purity in high and low risk group in CGGA1 (A) and CGGA2 (B) dataset. Immunocytes infiltration ratio in CGGA1 (C) and CGGA2 (D) dataset. The correlation between immunocytes enrichment score and risk in CGGA1 (E) and CGGA2 (F) dataset. NS, not significant, \* $p < 0.05$ , \*\* $p < 0.01$ , \*\*\* $p < 0.001$ .

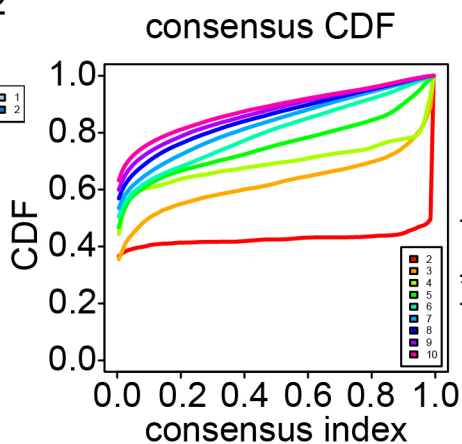
**Supplementary figure 5.** Univariate and multivariate Cox regression. Univariate and multivariate Cox regression in the TCGA (A-B), CGGA1 (C-D), CGGA2 (E-F) dataset.



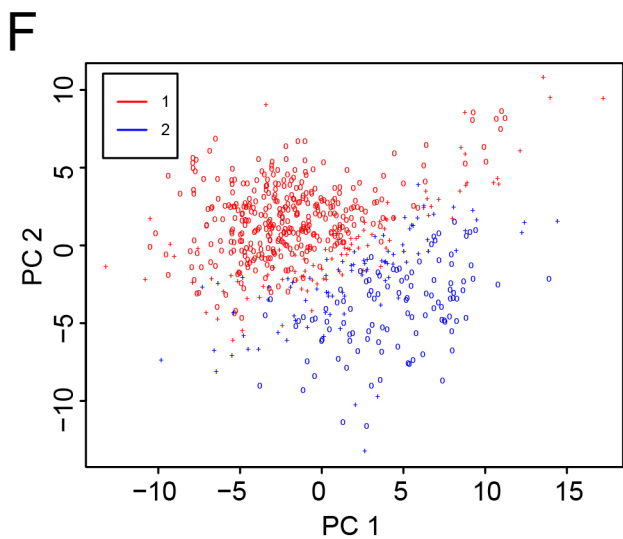
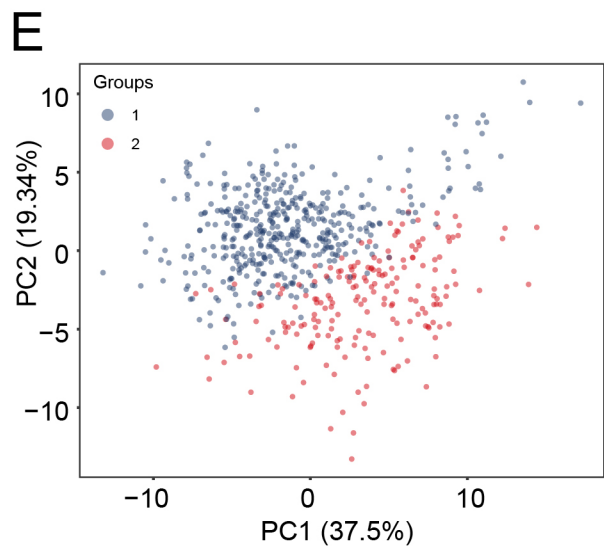
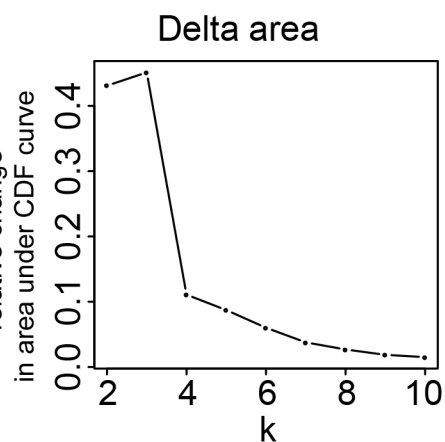
**B**  
consensus matrix k=2

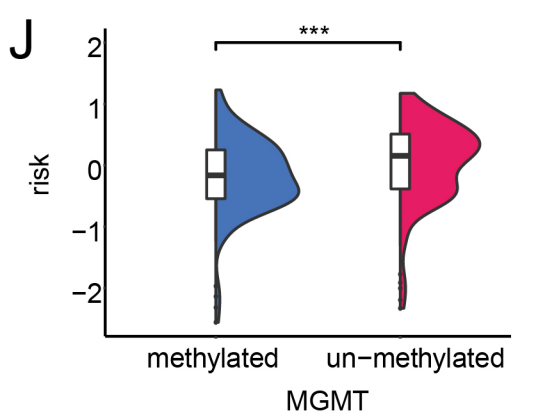
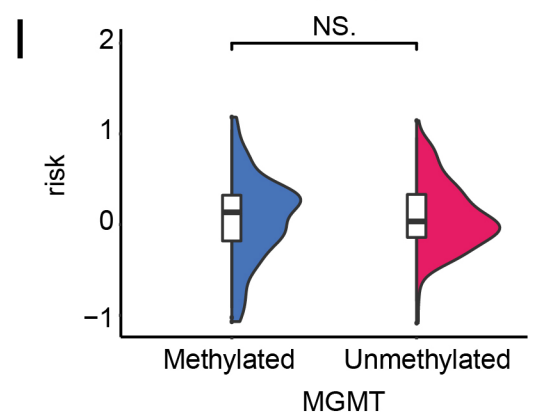
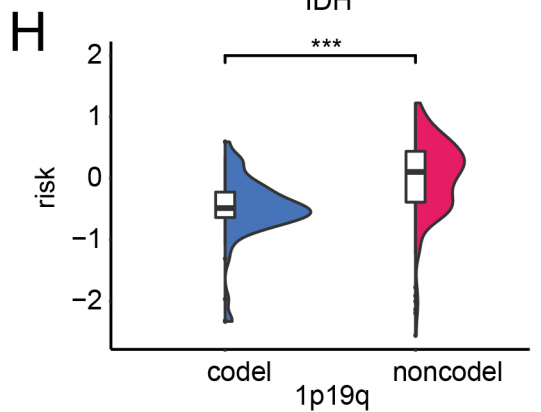
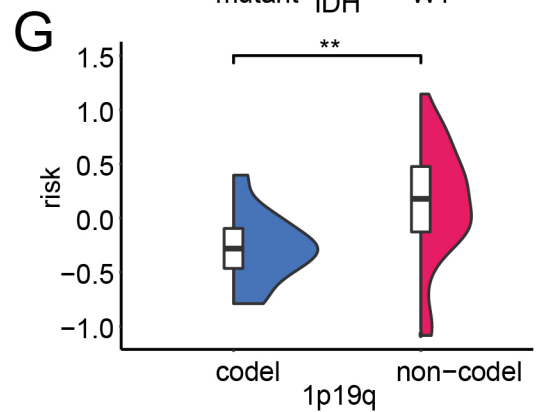
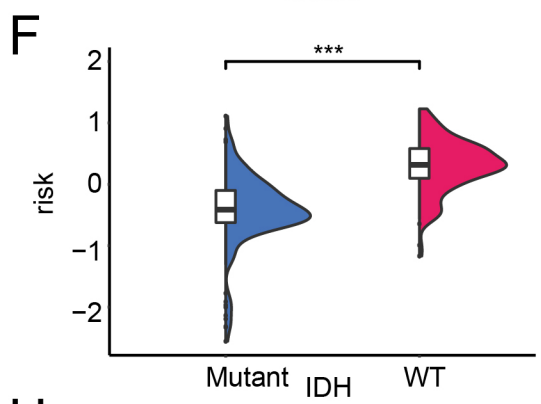
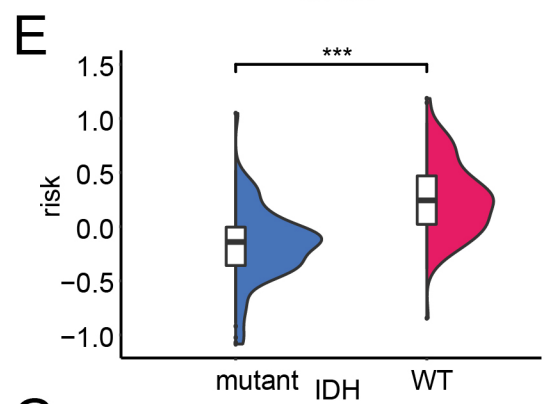
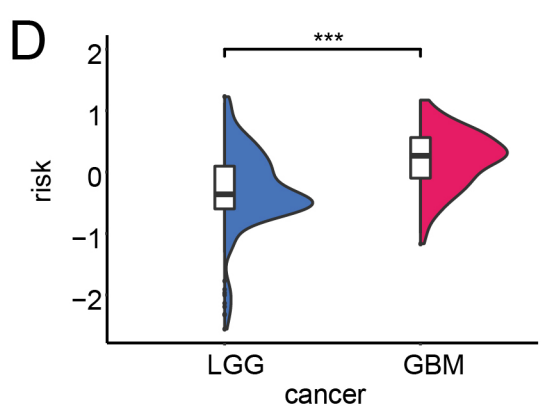
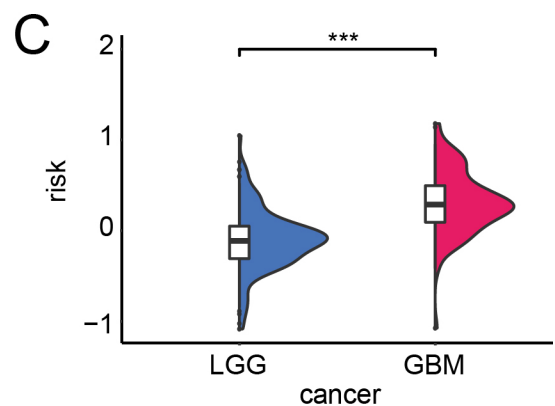
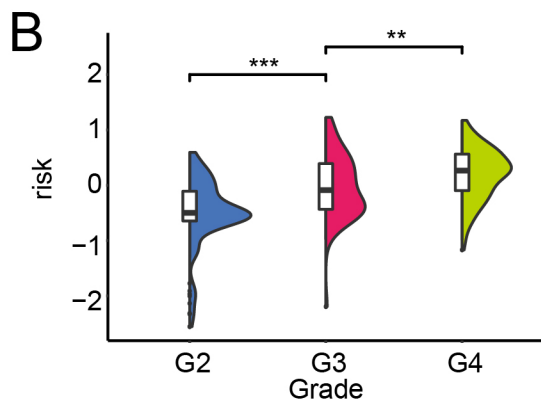
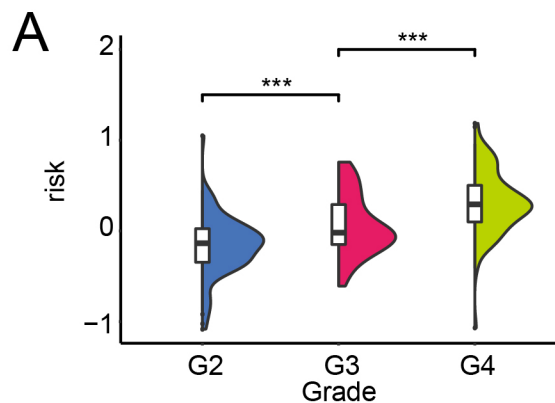


**C**



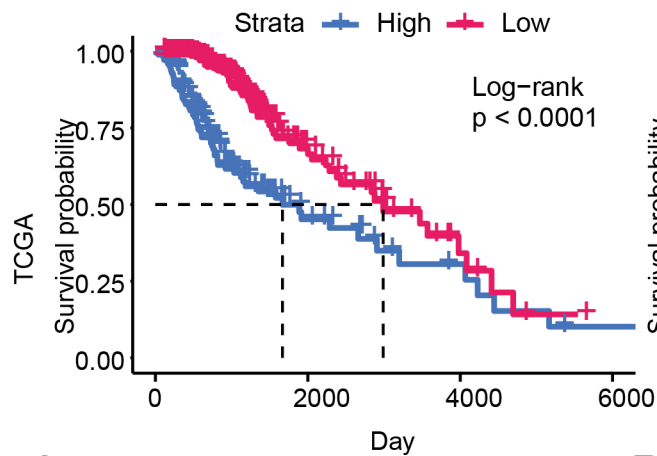
**D**



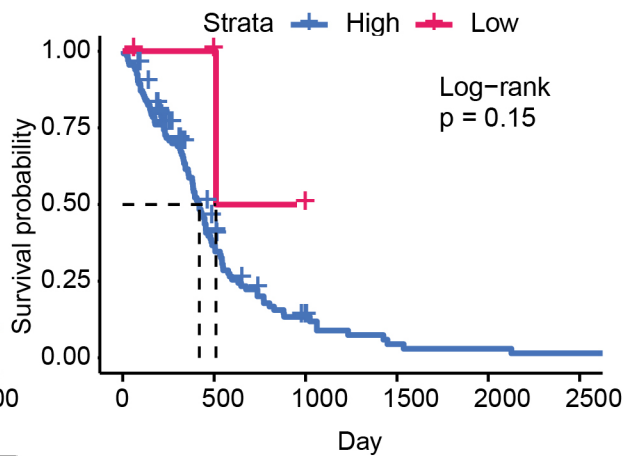
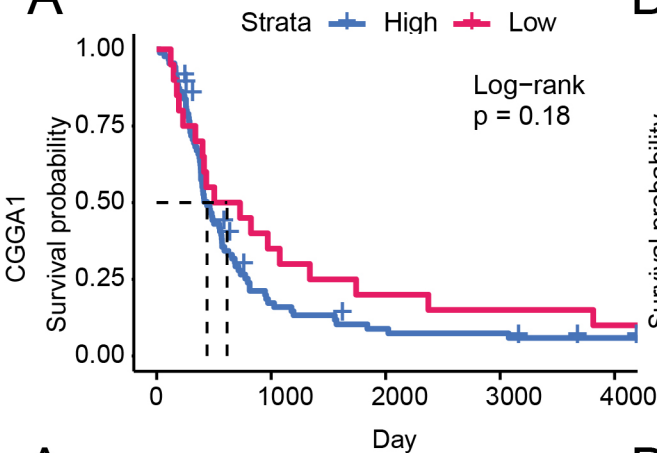
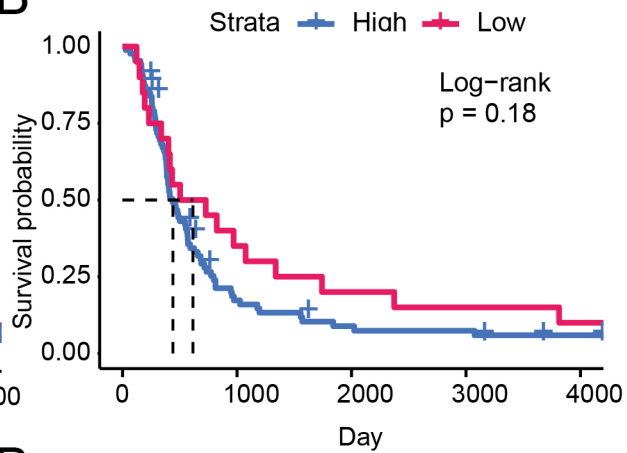
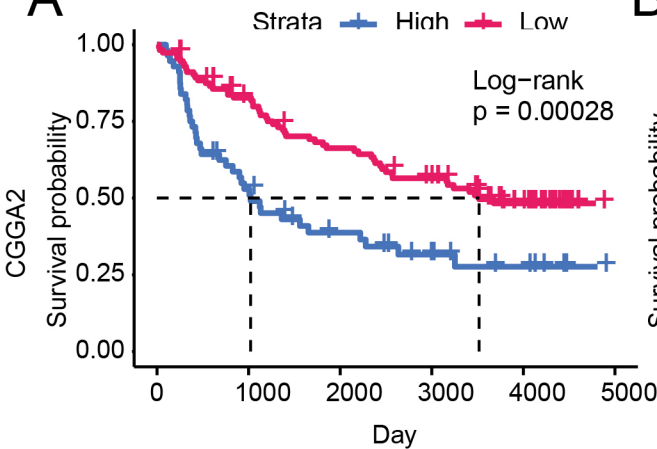


**A**

LGG

**B**

GBM

**A****B****A****B**